Monatshefte für Chemie - Chemical Monthly (2023) 154:497–502
https://doi.org/10.1007/s00706-023-03037-8

ORIGINAL PAPER

Synthesis of poly(*n*-alkyl acrylamides) and evaluation of nanophase separation effects by temperature-dependent infrared spectroscopy

Felix Leibetseder[1] · Julia Bičvić[1] · Klaus Bretterbauer[1]

Received: 25 October 2022 / Accepted: 8 January 2023 / Published online: 25 January 2023

Abstract

Common linear polymers are known to undergo phase changes at the glass-transition temperature (T_g) and the melting point (T_m). In recent years, it has also been shown that molecules with long aliphatic side chains can give rise to a backbone-independent melting phenomenon, known as nanophase separation. This effect describes the self-assembly — independent of the polymer backbone — of alkyl side chains into semi-crystalline nanostructures. This work presents optimized, gram scale synthesis routes for dodecyl and octadecyl acrylamide and their respective homopolymers. Differential scanning calorimetry (DSC) experiments detected a broad endothermal signal for poly(*n*-dodecyl acrylamide) at − 29 °C and a narrower, more intense signal for poly(*n*-octadecyl acrylamide) at 34 °C. These signals indicate the nanophase separation T_M of the alkyl side chains. We undertook the first temperature-controlled infrared spectroscopy investigations of these materials revealing a clear hypsochromic shift of the C–H stretching signals above T_M and the amide I signal shifts that occurred only above and below T_g. These results provide further evidence, that the side chains act independently of the polymer backbone and show that infrared spectroscopy is a powerful tool for monitoring conformational changes in polymer side chains.

Graphical abstract

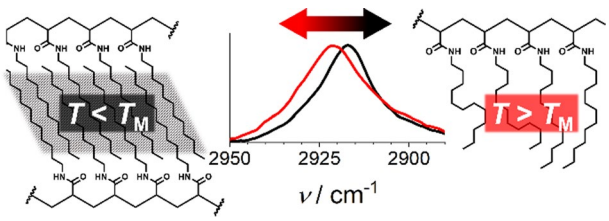

Keywords Polymerizations · IR spectroscopy · Nanostructures · Conformational analysis · Side-chain crystallization

Introduction

Rehberg and Fisher [1] first synthesized and described poly(*n*-alkyl acrylates) and discovered that polymers with longer aliphatic side chains show very unique thermal properties. In contrast to semi-crystalline polymers, which exhibit glass transition (T_g) and melting of the polymer backbone (T_m), these materials additionally show melting of the side chains (T_M) [2–4]. Long aliphatic side chains that form semi-crystalline polyethylene-like nanodomains are responsible for this peculiar thermal behavior [5]. These special properties are also found in poly(*n*-alkyl methacrylate) [1] as well as poly(*n*-alkyl acrylamide) [2]. Homo- and co-polymers that show nanophase separation effects have been investigated for many different applications, including gas-permeation membranes [6–9], Langmuir–Blodgett films [10–12], shape-memory polymers [13–16], and adhesive modifiers [17], and in other contexts in which their phase-change behavior is useful [18–20].

n-Dodecyl acrylamide (**1**) has the minimum chain length required to exhibit this phenomenon in poly(*n*-alkyl acrylamide), with a T_M of around − 30 °C [4, 21]. The side-chain

✉ Klaus Bretterbauer
klaus.bretterbauer@jku.at

[1] Institute for Chemical Technology of Organic Materials, Johannes Kepler University Linz, Linz, Austria

Scheme 1

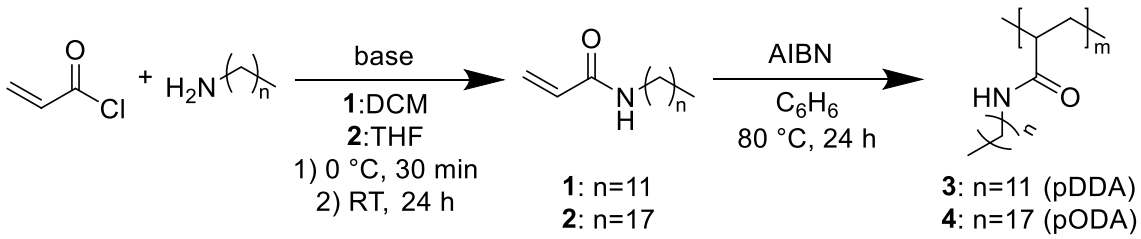

melting temperature rises with longer chains, and for *n*-octadecyl acrylamide (**2**) it is 32 °C according to the literature [21, 22]. Side-chain melting and crystallization have been studied mainly by means of differential scanning calorimetry (DSC) [4, 23–26], dielectric spectroscopy [3, 23], and X-ray diffraction measurements [3, 4, 21, 25–27]. As pointed out by Hashimoto et al. [4], the conformations of the backbone and the side chains can be additionally elucidated via the amide I and C–H stretching IR-regions. Depending on the exact shift of the signals, various different (side)chain conformations can be detected.

Here, we present optimized multi-gram scale synthesis procedures for *n*-dodecyl- and *n*-octadecyl acrylamides and their homopolymers. Additionally, we describe for the first time the detection of significant IR-shifts at temperatures above and below the T_M values of poly(*n*-dodecyl acrylamide) (**3**, pDDA) and poly(*n*-octadecyl acrylamide) (**4**, pODA) from which changes in their nanophase microstructures can be deduced.

Results and discussion

Synthesis of the monomers and polymers

n-Alkyl acrylamides are conventionally obtained through the reaction of an aliphatic primary amine with acryloyl chloride in the presence of a base. Multiple publications [21, 25, 28–31] have described the acrylamides **1** and **2**, synthesized mostly in small-scale and with multi-step work-up procedures. We modified and improved the synthesis procedures, to make them robust and effective in yielding high-purity products. Compound **1** was synthesized with a second equivalent of *n*-dodecyl amine rather than by adding triethylamine as the hydrogen chloride scavenger [28]. This improves the purity of the product, because no side products could form by reaction of acryloyl chloride with triethylamine or its impurities. Recrystallization from acetone was the only — and easily upscalable — purification step, which provided a 69% yield of acrylamide **1**, with a purity greater than 99% as determined by high-performance liquid chromatography (Scheme 1). The byproduct *n*-dodecyl amine hydrochloride can be conveniently recycled (96%) by treatment with aqueous NaOH solution and a single extraction step. A second extraction step allows quantitative recovery of *n*-dodecyl amine.

In contrast to the preparation of **1**, synthesis of the sparingly soluble acrylamide **2** benefitted from the use of triethylamine (Scheme 1). The reaction is carried out directly in tetrahydrofuran (THF) rather than in dichloromethane (DCM) [25]. This eliminated an unnecessary solvent evaporation step and improved purity of the crude product obtained by simple filtration. Single recrystallization from methanol afforded pure **2** (according to ^{1}H NMR).

The homopolymers pDDA (**3**) and pODA (**4**) were synthesized by classical free radical polymerization initiated with AIBN at 80 °C (Scheme 1). This led to polymers with number-average molecular weights of 11.4 kg mol^{-1} for **3** and 16.1 kg mol^{-1} for **4** and polydispersities of 5.1 and 3.6, respectively. The polymerization reactions achieved levels of monomer conversion greater than 90%. Thermal analysis of the polymeric materials with DSC revealed the unusual phenomenon of nanophase side-chain crystallization — a glass transition above the melting signal (Fig. 1).

In the case of pDDA (**3**) (see Fig. 1a), this effect is visible as a weak endothermal signal at − 29 °C (Fig. 1a), which matches values reported in the literature [4, 21]. The side-chain crystallization effect becomes more pronounced with longer alkyl chains resulting in a strong melting signal at 34 °C (Fig. 1b), which is also in agreement with published values [21, 22]. However, Hempel et al. [26] pointed out, the exact values of T_M can shift depending on the preceding crystallization process.

Unlike for common linear polymers, T_g was found above the melting temperature. Glass transition was identified at 77 °C for pDDA (**3**) and at 68 °C for pODA (**4**). The similarity of the T_g values is due to the two polymers having the same acrylamide backbone. The values obtained indicate backbone-independent melting of the alkyl side-chain nanodomains.

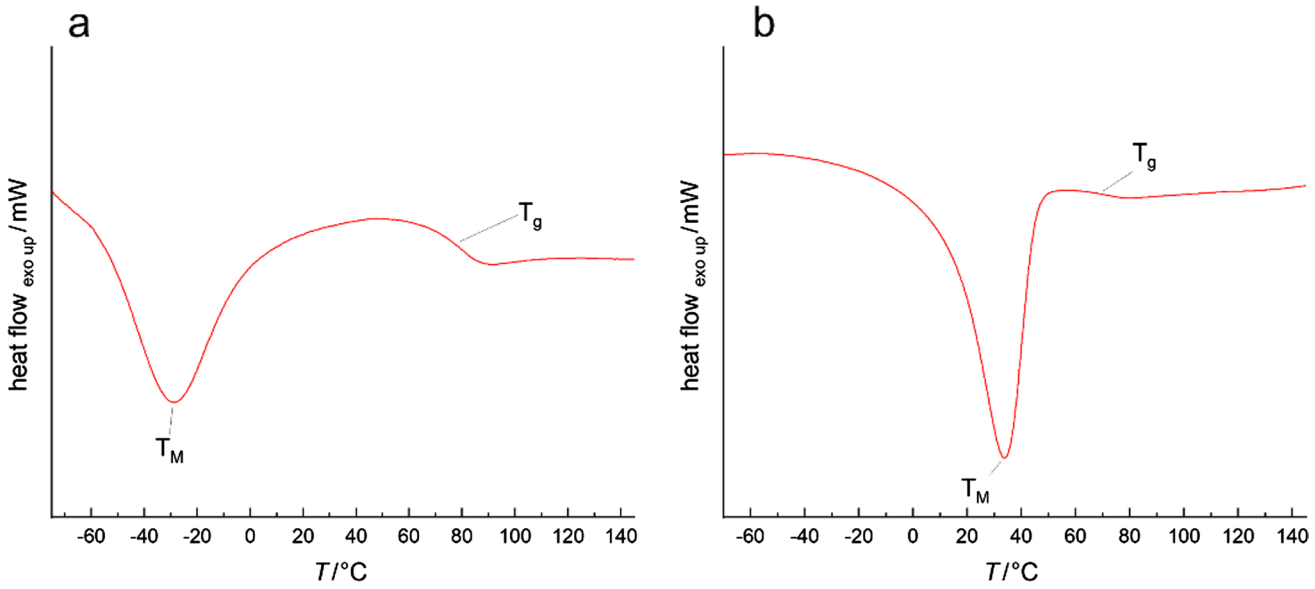

Fig. 1 DSC-thermogram of (**a**) pDDA (**3**) showing a broad weak endothermal signal T_M with a maximum at − 29 °C and a T_g at 77 °C. Thermogram (**b**) of pODA (**4**) shows a strong endothermal signal T_M at 34 °C and a discrete T_g at 68 °C. Both thermograms were recorded after a heat-cool-heat cycle at a heating rate of 10 °C min^{-1} after a 10 min hold at − 80 °C

Temperature-controlled ATR-FTIR analysis

This study was the first to use temperature-controlled attenuated total reflection Fourier-transform infrared spectroscopy (ATR-FTIR) to investigate side-chain melting. Figure 2a, c shows the FTIR spectrum of polymer **4** at room temperature (solid black) and at 100 °C (dashed red). The asymmetric and symmetric C–H stretching signals (Fig. 2a) show a clear hypsochromic shift of about 4 cm^{-1} (± 1 cm^{-1}) above and below the T_M. The exact maxima of this signal can give insights into the conformation of methylene groups of the polymer side chains. A fully ordered all-*trans zigzag* conformation would show signals at 2918 cm^{-1} and 2848 cm^{-1} (± 1 cm^{-1}), while more disordered chains would show a hypsochromic shift toward 2927 cm^{-1} and 2856 cm^{-1} [4, 32]. Thus, the shift from 2917 cm^{-1} to 2921 cm^{-1} (Fig. 2a) is related to a conformational change caused by side-chain melting and crystallization. Additionally, a change in the C–H bending signal at 1466 cm^{-1} can be seen in Fig. 2c. Similar behavior was exhibited by polymer **3** (Fig. 2b). The sample was measured below the determined T_M of − 29 °C (dash–dotted blue), above the T_M and below the T_g at room temperature (25 °C, solid black) and above the T_g at 100 °C (dashed red). When the polymer was cooled below T_M, a less pronounced but detectable hypsochromic shift of 2–3 cm^{-1} occurred.

The amide I region shown in Fig. 2c, d exhibits signal shifts due to a glass-transition phase change. The amide I signals at 1645 cm^{-1} and 1540 cm^{-1} are attributed to C=O stretching and the in-plane N–H bend of the secondary amide, respectively. Most importantly, the pDDA (**3**) results (Fig. 2d) demonstrate that the amide I region changes only above and below the T_g and remains unchanged above and below the T_M. Thus, the side-chain nanophase separation was independent of the polymer backbone. The temperature-dependent signal shifts detected were fully reversible. Intermediate temperature measurements showed that shifts occurred only directly above and below T_M and T_g. No gradual shifts were observed between the phase-change temperatures and were, therefore, omitted in Fig. 2 to improve clarity.

Temperature-controlled FTIR analysis is a fast and convenient new method for detecting and monitoring the side-chain melting of brush polymers. The conformations of polymer side-chain and backbone at different temperatures can thus be estimated, which allows tailored polymer synthesis. The temperature-dependent FTIR measurements presented here corroborate X-ray diffraction [3, 4, 21, 25–27] and DSC [4, 23–26] data reported in the literature.

Conclusion

The acrylamides **1** and **2** were successfully synthesized with high purity at multi-gram scale by improved, straightforward procedures. The polymers prepared — pDDA (**3**) and pODA (**4**) — exhibited side-chain melting and crystallization behavior, detected by DSC. This is the first capturing of a nanophase separation phenomenon by temperature-dependent ATR-FTIR. The change between ordered

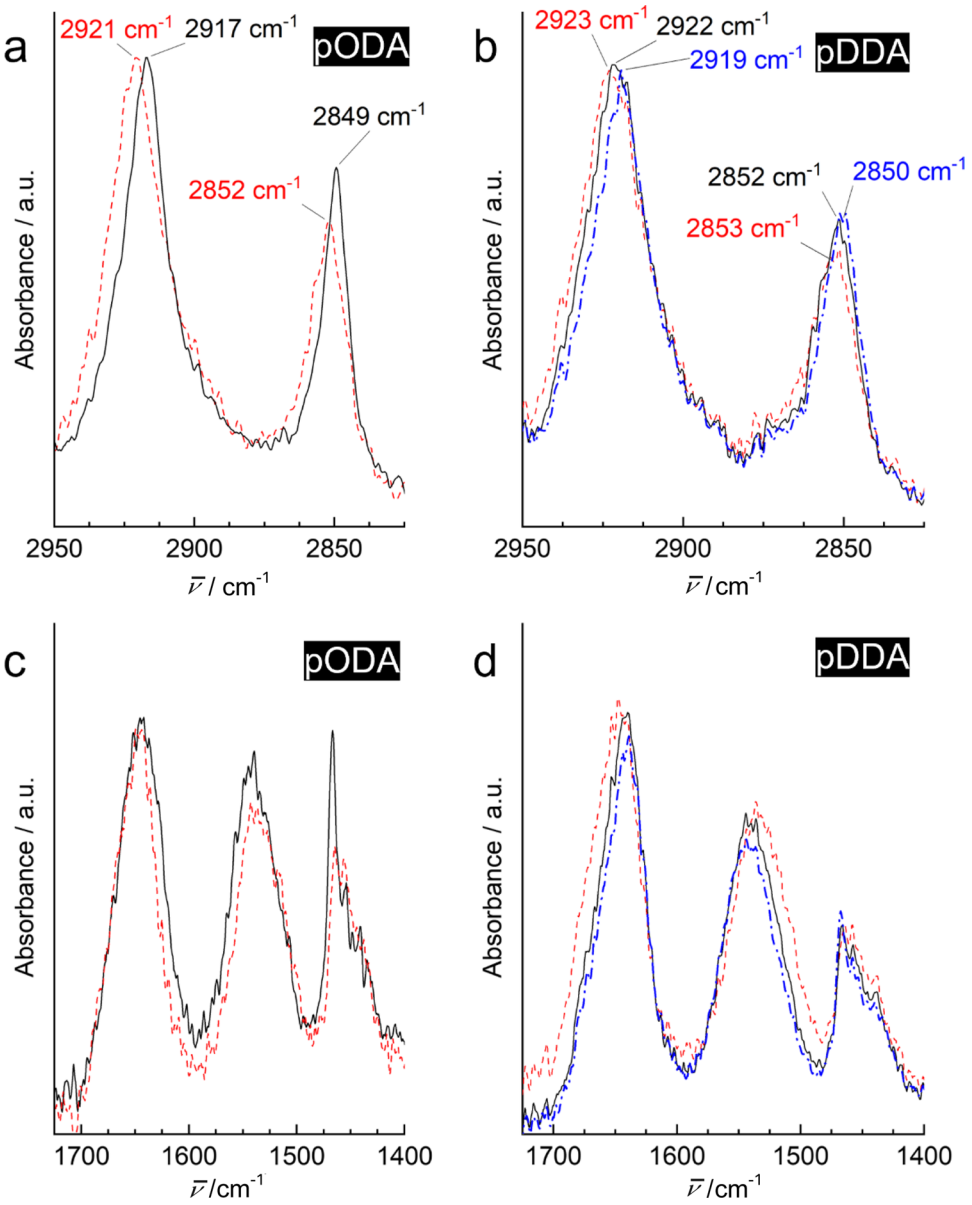

Fig. 2 ATR-FTIR absorbance spectra measured at various temperatures. Spectra (**a**, **b**) show the C–H symmetric and asymmetric stretching signals, while (**c**, **d**) show the amide I IR region. (**a**, **c**) show the measurement of pODA (**4**). (**b**, **d**) display the measurement of pDDA (**3**). All measurements were made at room temperature (25 °C, solid black) and 100 °C (dashed red) and below the T_M (dash dotted blue) for pDDA (**3**) (color figure online)

and disordered alkyl side-chain conformation above and below the T_M, caused a measurable hypsochromic 4 cm^{-1} shift of the asymmetric and symmetric C–H stretching signals. The shift detected confirms the nanophase separation of the alkyl side chains. The information obtained from the amide I region provides additional proof of polymer-backbone-independent side-chain behavior. IR signal shifts occurred directly around the phase-change temperatures and were fully reversible. Temperature-dependent ATR-FTIR spectroscopy is a new and convenient measurement procedure for detecting and monitoring side-chain crystallization phenomena in advanced functional polymeric materials.

Experimental

All reagents and solvents used were purchased from standard chemical suppliers in reagent quality and were used without further purification. All NMR spectra were recorded in $CDCl_3$ on a 300 MHz Bruker Avance spectrometer using standard pulse programs as provided by the manufacturer. Signals were referenced to the solvent signal at 7.26 ppm (^{1}H) and 77.0 ppm (^{13}C). High-resolution mass spectra were recorded on a LTQ Orbitrap Velos with positive mode electrospray ionization (ESI). Gel permeation chromatography of the polymers was performed at 40 °C in THF on an Agilent Technologies 1200 Series device equipped with one Phenomenex guard column SecurityGuard™ and three Phenomenex Phenogel™ 5 µm columns 10^3 Å, 10^4 Å,

and 10^5 Å. A Waters 410 Differential Refractometer was employed for detection and the system was calibrated with polystyrene standards. A Mettler Toledo DSC 3 + equipped with a TC 100 IntraCooler was used for thermal analysis of the polymers. Heat-cool-heat cycles between − 80 °C and 150 °C were performed. T_g and T_M were determined at a heating rate of 10 °C min^{-1} after an isothermal hold step of 10 min at − 80 °C. Fourier-transform infrared spectroscopy was performed on a Thermo Electron Nicolet 5700 spectrometer with a Specac Golden Gate High Temperature Attenuated Total Reflectance (ATR) sampling unit. For low-temperature measurements, a weighed-down metal crucible filled with liquid nitrogen was placed on top of the sample. For each measurement, 128 scans were recorded at a resolution of 1.0 cm^{-1} and a data spacing of 0.482 cm^{-1}.

***n*-Dodecyl acrylamide (1)** A solution of 15.7 g of *n*-dodecyl amine (84.7 mmol) in 250 cm^3 of dichloromethane was cooled in an ice bath and 4.0 cm^3 of acryloyl chloride (49.1 mmol) in 30 cm^3 of dichloromethane was added dropwise, and the resulting suspension was stirred overnight at room temperature. The white *n*-dodecyl amine hydrochloride precipitate was removed by filtration. The filtrate was dried under reduced pressure to afford the crude product. Purification was achieved by recrystallization from acetone. After drying under vacuum *n*-dodecyl acrylamide (**1**) was obtained as an off-white solid with a yield of 7.00 g (69%). M.p.: 56.5 °C (Ref [28] 54–55 °C); ^{1}H NMR (300 MHz, $CDCl_3$): $\delta = 6.27$ (dd, $J_1 = 17.0$ Hz, $J_2 = 1.6$ Hz, 1H, CH), 6.07 (*dd*, $J_1 = 17.0$ Hz, $J_2 = 10.1$ Hz, 1H, CH_2), 5.64–5.58 (m, 2H, CH_2 and NH), 3.32 (dt, $J_1 = 6.0$ Hz, $J_2 = 7.1$ Hz, 2H, CH_2), 1.55–1.48 (m, 2H, CH_2), 1.29–1.25 (m, 18H, CH_2), 0.87 (t, $J = 6.9$ Hz, 3H, CH_3) ppm; ^{13}C NMR (APT, 75 MHz, $CDCl_3$): $\delta = 165.4$, 131.1, 126.0, 39.6, 31.9, 29.6, 29.6, 29.5, 29.5, 29.3, 29.3, 26.9, 22.6, 14.1 ppm; FTIR (ATR): $\tilde{\nu} = 3263$, 2971, 2958, 2920, 2848, 1651, 1620, 1551, 1475, 1406, 1244, 993, 966, 810 cm^{-1}; MS (ESI): $m/z = 240.238$ ($[M + H]^+$).

Recycling of *n*-dodecyl amine

5.0 g (22.5 mmol) of *n*-dodecyl amine hydrochloride, accumulating as a precipitate in the synthesis of **1**, was suspended in 50 cm^3 of 1 M NaOH solution and stirred at room temperature for 10 min. The suspension was then extracted once with 30 cm^3 of dichloromethane. Evaporation of the organic phase and drying in vacuo yielded 4.0 g of *n*-dodecyl amine (21.6 mmol, 96%) as a white solid. A second extraction step with 30 cm^3 of dichloromethane gives quantitative yields. The product obtained was directly reused in the synthesis of **1** without further purification.

***n*-Octadecyl acrylamide (2)** 8.33 g of *n*-octadecylamine (30.9 mmol) and 4.5 cm^3 of triethylamine (32.5 mmol) were dissolved in 250 cm^3 of THF. Acryloyl chloride (3.0 cm^3, 36.8 mmol) in 30 cm^3 of THF was added dropwise under ice cooling over a period of 30 min, and the resulting suspension was stirred overnight at room temperature. The crude product was isolated by filtration, dried and recrystallized from methanol. 7.72 g of *n*-octadecyl acrylamide **2** (77%) was obtained as a white solid. M.p.: 72.9 °C (Ref. [33] 73.5–74.0 °C); ^{1}H NMR (300 MHz, $CDCl_3$): $\delta = 6.27$ (dd, $J_1 = 17.0$ Hz, $J_2 = 1.6$ Hz, 1H, CH), 6.07 (dd, $J_1 = 17.0$ Hz, $J_2 = 10.2$ Hz, 1H, CH_2), 5.65–5.56 (m, 2H, CH_2/NH), 3.33 (dt, $J_1 = 6.0$ Hz, $J_2 = 7.1$ Hz, 2H, CH_2), 1.56–1.51 (m, 2H, CH_2), 1.30–1.25 (m, 30H, CH_2), 0.88 (t, $J = 6.9$ Hz, 3H, CH_3) ppm; ^{13}C NMR (APT, 75 MHz, $CDCl_3$): $\delta = 165.4$, 131.0, 126.1, 39.6, 31.9, 29.7–29.3, 26.9, 22.7, 14.1 ppm; IR (ATR): $\tilde{\nu} = 3149$, 2804, 2765, 2700, 1504, 1475, 1387, 1257, 1088, 839, 800 cm^{-1}; MS (ESI): $m/z = 324.336$ ($[M + H]^+$).

Poly(*n*-dodecyl acrylamide) (3) A 0.20 M monomer solution was prepared by dissolving 5.0 mmol of **1** in 25.0 cm^3 of benzene. The solution was subsequently purged with nitrogen for 30 min and then heated to reflux, and polymerization was initiated with 0.5 cm^3 of a 0.10 M 2,2′-azobis(2-methylpropionitrile) solution in benzene. After refluxing for 24 h, the solvent was removed by rotary evaporation and the poly(*n*-dodecyl acrylamide) pDDA (**3**) obtained was dried in vacuo and used without further purification. C = 95%; $M_n = 11{,}400$ g mol^{-1}; $Đ_M = 5.1$.

Poly(*n*-octadecyl acrylamide) (4) Poly(*n*-octadecyl acrylamide) pODA (**4**) was synthesized analogously to pDDA (**3**). $C = 94\%$; $M_n = 16{,}100$ g mol^{-1}; $Đ_M = 3.6$.

Acknowledgements The authors gratefully thank Prof. Dr. Christian Paulik for fruitful discussions and Assoc. Prof. Dr. Clemens Schwarzinger for assistance with ATR-FTIR and HRMS measurements. The NMR spectrometer was acquired in collaboration with the University of South Bohemia (CZ) with financial support from the European Union through the EFRE INTERREG IV ETC-AT-CZ program (project M00146, "RERI-uasb").

Funding Open access funding provided by Johannes Kepler University Linz.

Data Availability All data generated or analyzed during this study are included in this published article.

References

1. Rehberg CE, Fisher CH (1944) J Am Chem Soc 66:1203
2. Jordan EF, Feldeisen DW, Wrigley AN (1971) J Polym Sci A Polym Chem 9:1835
3. Beiner M, Huth H (2003) Nat Mater 2:595
4. Hashimoto Y, Sato T, Goto R, Nagao Y, Mitsuishi M, Nagano S, Matsui J (2017) RSC Adv 7:6631
5. Beiner M (2001) Macromol Rapid Commun 22:869
6. Semsarzadeh MA, Ghahramani M (2020) J Membr Sci 594:117400
7. Paul DR, Clarke R (2002) J Membr Sci 208:269
8. Mogri Z, Paul D (2001) Polymer 42:2531
9. Lee J-W, Kim H-T, Park J-K, Lee K-H (2000) J Membr Sci 167:67
10. Miyashita T, Suwa T (1994) Langmuir 10:3387
11. Miyashita T, Yoshida H, Murakata T, Matsuda M (1987) Polymer 28:311
12. Miyashita T, Sakaguchi K, Matsuda M (1992) Langmuir 8:336
13. Kagami Y, Gong JP, Osada Y (1996) Macromol Rapid Commun 17:539
14. Lin XK, Chen L, Zhao YP, Dong ZZ (2010) J Mater Sci 45:2703
15. Tian Y, Du C, Liu B, Qiu HN, Zhang X-H, Wu ZL, Zheng Q (2021) J Polym Sci 59:904
16. Matsuda A, Sato J, Yasunaga H, Osada Y (1994) Macromolecules 27:7695
17. Agirre A, Nase J, Degrandi E, Creton C, Asua JM (2010) J Polym Sci A Polym Chem 48:5030
18. Qu M, Wang H, Zheng N, Chen Q, Tang P, Bin Y (2022) J Appl Polym Sci 139:51794
19. Gao M, Meng Y, Shen C, Pei Q (2022) Adv Mater 34:e2109798
20. Lee J-W, Park J-K, Lee K-H (2000) J Polym Sci B Polym Phys 38:823
21. Ebata K, Hashimoto Y, Yamamoto S, Mitsuishi M, Nagano S, Matsui J (2019) Macromolecules 52:9773
22. Kunisada H, Yuki Y, Kondo S, Wada K (1991) Polym J 23:1365
23. Hempel E, Huth H, Beiner M (2003) Thermochim Acta 403:105
24. Hempel E, Beiner M, Huth H, Donth E (2002) Thermochim Acta 391:219
25. Kametani Y, Tournilhac F, Sawamoto M, Ouchi M (2020) Angew Chem Int Ed 59:5193
26. Hempel E, Budde H, Höring S, Beiner M (2006) J Non-Cryst Solids 352:5013
27. Ebata K, Hashimoto Y, Ebara K, Tsukamoto M, Yamamoto S, Mitsuishi M, Nagano S, Matsui J (2019) Polym Chem 10:835
28. Wan W-M, Pickett PD, Savin DA, McCormick CL (2014) Polym Chem 5:819
29. Yamaguchi H, Kobayashi R, Takashima Y, Hashidzume A, Harada A (2011) Macromolecules 44:2395
30. Oh D, Furuya Y, Ouchi M (2019) Macromolecules 52:8577
31. Akinc A, Zumbuehl A, Goldberg M, Leshchiner ES, Busini V, Hossain N, Bacallado SA, Nguyen DN, Fuller J, Alvarez R, Borodovsky A, Borland T, Constien R, de Fougerolles A, Dorkin JR, Narayanannair Jayaprakash K, Jayaraman M, John M, Koteliansky V, Manoharan M, Nechev L, Qin J, Racie T, Raitcheva D, Rajeev KG, Sah DWY, Soutschek J, Toudjarska I, Vornlocher H-P, Zimmermann TS, Langer R, Anderson DG (2008) Nat Biotechnol 26:561
32. Zhang Z, Verma AL, Yoneyama M, Nakashima K, Iriyama K, Ozaki Y (1997) Langmuir 13:4422
33. Jordan EF, Wrigley AN (1964) J Appl Polym Sci 8:527